

# Five-fold symmetry in the hydrogen atom probed with accurate 1S-nS terms

G. Van Hooydonk, Ghent University, Faculty of Sciences, Ghent, Belgium

Abstract. We probe Penrose's five-fold symmetry in the hydrogen atom using its radius  $r_H$  as derived classically from its mass  $m_H$ . This generic H symmetry, obeying Euclid's golden ratio  $[\sqrt{5}-1]/2$  for its 2 constituent complementary parts, is confirmed with precise H terms. These give away a Hund-type Mexican hat curve for natural H, which points to its mirrored variant, antihydrogen  $\underline{H}$ . We predict that term H 1S-3S, to be measured soon, is 2 922 743 278 654(2) kHz.

## I. Introduction

Uncertainties with H CPT-symmetry resulted in attempts to produce antihydrogen  $\underline{H}$ , to measure its interval  $\underline{H}$  1S-2S and to compare this with H 1S-2S [1]. Instead of CPT, Euclidean symmetries also rationalize composite unit H. Euclidean numbers appear in many fields of science [2-3], for chaotic/fractal behavior (Mandelbrot [4], Gutzwiller [5]) and for Penrose 5-fold symmetry [6]. Whenever parts  $+x$  and  $(1-x)$  in unit 1 obey  $(1-x)/x=x/1$ , Euclidean symmetries  $x_{\pm}=\varphi_{\pm}=\frac{1}{2}(1\pm\sqrt{5})$  appear. Atom H, the simplest composite but most abundant unit in the Universe [7], has complementary parts electron ( $m_e$ ) and proton ( $m_p$ ):  $m_H=m_e+m_p=m_e+(m_H-m_e)$  or  $1=x+(1-x)$ , if  $x=m_e/m_H$ . If  $\varphi$  were relevant for H, it must show in its spectrum, although it is absent in QED [8]. We now probe  $\varphi$  for H using mass  $m_H$  and radius  $r_H$  in  $m_H=4\pi\gamma r_H^3/3$ . In line with Rydberg's formula [9], scaling H levels by  $\frac{1}{2}e^2/r_H$  gives away  $\varphi$  and fractal behavior with precise H 1S-nS terms [10]. We predict a value of 2922743278654(2) kHz for H 1S-3S, to be measured soon [11].

## II. Rydberg equation and fractal behavior of atom H

### II.1 Chaotic/fractal interpretation of the Rydberg formula for composite H

With constant  $a$  in  $\text{\AA}$  and line number  $n$ , the original Rydberg formula [9] for H terms

$$T_n=an^2/(n^2-1) \text{\AA} \text{ or } T_n/(an) = n/(n^2-1) = 1/(n-1/n) \quad (1)$$

suggests that H exhibits fractal/chaotic behavior [4,5]. Bohr energy differences

$$\Delta E_n=1/T_n = (n^2-1)10^8/(an^2) = R_H (1-1/n^2) = R_H - R_H/n^2 = E_n - E_1 \text{ cm}^{-1} \quad (2)$$

with Rydberg  $R_H=10^8/a \text{ cm}^{-1}$ , give the linear version of (1), i.e.

$$n\Delta E_n/R_H=(n-1)(n+1)/n=n-1/n \quad (3)$$

With  $E_n$  [12] instead of  $\Delta E_n$ , plots of  $nE_n$  versus  $n$  and  $1/n$  give power laws

$$E_n(n)\equiv E_n(1/n)=109679,223605211n^{-1,000004252339}\equiv 109679,223605211(1/n)^{1,000004252339} \quad (4)$$

Linear  $n$  and inverse  $1/n$  views on fractal H (1)-(3) give errors of only  $0,007 \text{ cm}^{-1}$ , while Bohr's are  $0,0126 \text{ cm}^{-1}$  (a power fit in  $1/n^2$  has its exponent shifted by 1). Fractal asymptote  $109679,2236 \text{ cm}^{-1}$  in (4) is much larger than in Bohr theory or QED, i.e.  $-E_1=109678,773704 \text{ cm}^{-1}$  [12], to which we return in Section V. Since  $1/n$  secures convergence, a 4<sup>th</sup> order fit in  $1/n$

$$nE_n=0,006889343262/n^4-4,375765800476/n^3+5,5580713748932/n^2+109677,585385323000/n \quad (5)$$

is accurate within  $10^{-8} \text{ cm}^{-1}$  or 0,45 kHz (less precise data [13] behave similarly). By its precision, (5) must be important for H-based metrology [10, 14-15].

## II.2 Generalized Bohr H theory and reduced mass: opening for $\varphi$

To not to interrupt the argument on  $\varphi$ , we compare H theories in Appendix A. With (A1)-(A2), Bohr's integer quantum number  $n$  and Rydberg  $R_H$  give rotational level energies

$$E_n = -R_H/n^2 = -1/2(\hbar^2/\mu e^2)/n^2 = -1/2\mu\alpha^2 c^2/n^2 = -1/2(e^2/r_0)/n^2 \quad (6)$$

Here,  $r_0$  is Bohr radius  $r_B = \hbar^2/(m_e e^2)$ , corrected for reduced electron mass  $\mu$ , according to

$$\mu = m_e m_p / (m_e + m_p) = m_e m_p / m_H = m_e / (1 + m_e / m_p) \equiv m_e (1 - m_e / m_H) \quad (7)$$

Generalizing (6) with a critical  $n$ -value  $n_c$  for another H radius  $r_H$  gives respectively

$$r_H = n_c^2 r_0 \quad (8)$$

$$E_n = -(R_H/n_c^2)(n_c/n)^2 = -1/2(e^2/r_H)(n_c/n)^2 \quad (9)$$

(i) Any critical  $n_c$  ( $\neq 0$ ) will lead to the same accuracy as (6). A relation between  $n_c$  and  $\varphi$  like

$$n_c = A\varphi^m \quad (10)$$

plugged in (9), may probe Euclidean symmetry but only if an alternative  $r_H$  really existed (see Section II.3). If not, both (8) and (9) are trivial.

(ii) Detecting internal  $\varphi$ -effects in H depends on specific  $\varphi$ -relations [2-3] like

$$\varphi^{m+2} + \varphi^{m+1} = \varphi^m; \quad 1 = 1/\varphi - \varphi; \quad \varphi^2 + \varphi - 1 = 0 \text{ and } \varphi(\varphi+1) = 1 \quad (11)$$

Internal  $\varphi$ -symmetries (11) are available from dimensionless (7). Scaling by  $m_H$  gives product

$$\varrho_H = \mu/m_H = (m_e/m_H)(1 - m_e/m_H) = x(1-x) \quad (12)$$

for parts. Here,  $d\varrho/dx = 1-2x=0$  gives  $\varrho_{\max} = 1/4$  for equal parts  $x=1/2$ , while  $\varrho = x(1-x)$  or  $x^2 - x + \varrho = 0$  gives  $x_{\pm} = 1/2[1 \pm \sqrt{1-4\varrho}]$ . A center between parts gives  $-x$ ,  $(1-x)$ ,  $x^2 - x + \varrho = 0$  and  $x_{\pm} = 1/2[1 \pm \sqrt{1+4\varrho}]$ .

Part ratios (12) secure all symmetries in (ii) are Euclidean. With  $\varrho_{\max} = 1/4$  and (10), we further get

$$\varrho_H = x(1-x) \sim A\varphi^m(1-A\varphi^m) \text{ and } \Delta\varrho = \varrho_{\max} - \varrho = 1/4 - x(1-x) = 1/4(1-2x)^2 \sim 1/4(1-2A\varphi^m)^2 \quad (13)$$

i.e. a parabola for  $\varphi$ -symmetries, with small corrections to  $E_n$ , since  $\mu/m_e$  in (7) is  $1837(\mu/m_e)$ . The fate of parabolic  $\varphi$ -symmetry (13) for H depends on the reality of a valid alternative radius  $r_H$ .

## II.3 Alternative classical H radius $r_H$

Apart from [16], a first principles alternative quantum radius for H, other than Bohr length  $r_B$ , does not exist. Only a classical 19<sup>th</sup> century macroscopic view on spherical H can give  $r_H$  using

$$m_H = (4\pi/3)\gamma r_H^3 \text{ and } r_H = [(3/4\pi\gamma)m_H]^{1/3} \quad (14)$$

with form factor  $4\pi/3 \gamma$  in  $\text{g/cm}^3$  is H density, which fixes the external H symmetry (its form).

With  $m_H = m_e + m_p = 9,10938215 \cdot 10^{-28} + 1,672621637 \cdot 10^{-24} \text{ g}$  [10] and  $\gamma = 1 \text{ g/cm}^3$  for H, the result is

$$r_H = 7,36515437 \cdot 10^{-9} \text{ cm} = 0,736515437 \text{ \AA} \quad (15)$$

This is the only real, theoretically plausible alternative to Bohr length  $r_B = 0,529177209 \text{ \AA}$  [16].

In (6), H radius  $r_0$  is Bohr length  $r_B$ , corrected for recoil (7) or

$$r_0=[\hbar^2/(m_e e^2)](1+m_e/m_p)=0,5294654075 \text{ \AA} \quad (16)$$

The ratio of classical natural H radius  $r_H$  in (15) and Bohr's  $r_0$  in (16) is

$$x=r_H/r_0=1,391054876... \quad (17)$$

(without recoil,  $r_H/r_B = 1,391812469...$ ).

The natural virial Coulomb energy  $-1/2e^2/r_H$  for any two charge-conjugated parts amounts to

$$1/2e^2/r_H=78844,900590508 \text{ cm}^{-1}=2363710654879,4 \text{ kHz} \quad (18)$$

### III. Scaling $E_n$ by $1/2e^2/r_H$ : probing five-fold or $\varphi$ -symmetry in atom H

Scaling  $E_n$  by natural H asymptote (18) gives numbers

$$N_n=[E_n/(1/2e^2/r_H)]/n^2 \text{ or } nN_n=[E_n/(1/2e^2/r_H)]/n \quad (19)$$

Due to (18), plots of  $nN_n$  versus  $1/n$  and  $(1-1/n)$  in Fig. 1 give 4<sup>th</sup> order fits (with 5 decimals)

$$N_n=-0,00006/n^4+0,00007/n^3+1,39106/n^2 \quad (20)$$

$$N_n=-0,000056(1-1/n)^4+0,00015(1-1/n)^3+1,39093(1-1/n)^2-2,78210(1-1/n)+1,39107 \quad (21)$$

With  $(1-1/n)$ , typical for molecular potentials [16], (20)-(21) reveal the effect of odd powers in  $1/n$ , absent in Bohr  $1/n^2$  theory and in a relativistic expansion in  $E_n=\mu c^2[1/\sqrt{(1+\alpha^2/n^2)}-1]$  [8,14].

In (A16)-(A17), we prove that the H *force constant*  $k_n$ , away from critical configuration  $n_c$ , varies with  $1,5/n$ . Fig. 1 includes  $N_n$  versus  $1,5/n$  and  $(1-1,5/n)$  with 5-decimal 4<sup>th</sup> order fits

$$N_n=-0,00001(1,5/n)^4+0,00002(1,5/n)^3+0,61825(1,5/n)^2 \quad (22a)$$

$$N_n=-0,00001(1-1,5/n)^4+0,00002(1-1,5/n)^3+0,61824(1-1,5/n)^2-1,23651(1-1,5/n)+0,61826 \quad (22b)$$

Coefficients of  $(1,5/n)^2$  in (22a) and  $(1-1,5/n)^2$  in (22b) are close to Euclid or Phidias number (10)

$$\varphi=1/2(\sqrt{5}-1)=1/\varphi-1=\Phi-1=0,618034 \quad \dots \quad (23)$$

Correction factor  $f_\varphi$  for external  $\varphi$ -symmetry and  $f_r$  for recoil (for an internal H-symmetry)

$$f_\varphi=0,618247/0,618034-1=0,000344; f_r=m_e/m_p=1/1836,15267247=0,000545 \quad (24)$$

shows that  $f_\varphi$  is smaller than  $f_r$  by 40 %. Difference  $\delta$  for  $\varphi$ -symmetry is 0,02 %, i.e.

$$\delta=0,618247-0,618034=0,000213 \quad (25)$$

In terms of ratio  $m_e/m_H=1/1837,15267247$  in (7), difference (25)

$$(m_H/m_e)0,000213=0,390635 \approx (9\varphi/4-1)=(9/4)(1/2\sqrt{5}-17/18) \quad (26)$$

reflects the importance of Euclid's golden ratio for H.

Combining coefficient for  $1,5/n$  (22a) and asymptote 0,618247 in (22a-b) gives ratio  $x$  in (18), since

$$x=(9/4) \cdot 0,618246619=(3/2)^2\varphi=1,391054894=r_H/r_0 \quad (27a)$$

Using (9), the Euclidean H variable  $x_E$  must therefore obey

$$x_E=a\varphi^{1/2}/n \quad (27b)$$

Results (21)-(27) probe Penrose's five-fold or Euclid's  $\varphi$ -symmetry in H, due to alternative classical radius  $r_H$  (15).

If external symmetry (27) also applied for internal H-symmetry according to (13), (27) prescribe Euclidean variable and symmetry parabola, given respectively by

$$X_E \sim x_E(1-x_E) \sim (\varphi^{1/2}/n)(\varphi^{1/2}/n-1) \text{ and } \Delta Q = Q_{\max} - Q \sim 1/4(1-2\varphi^{1/2}/n)^2 \quad (28)$$

whenever  $a=1$  in (27b). As shown previously [22], Euclidean symmetry parabola (28) appears in higher order for the H Lyman series  $1s-nS$  [12]. The phenomenological H parabola  $(1-1,572273/n)^2$  in [22] validates theoretical Euclidean H parabola (28), since  $2\varphi^{1/2}=1,572303$ . The difference with 1,572273 in [22] is only 0,002 %. We now verify whether precise H terms [17-21] confirm this early evidence [22] for 5-fold H symmetry (28).

#### IV. Accurate H intervals (prediction of H $1S_{1/2}$ - $3S_{1/2}$ )

The precision needed to validate (28) requires an upgrade of  $E_n$  [12], used in [22]. Table 1 shows the H terms available: 4 precisely known terms A, B, D and E give 2 derived terms C and F. Since only B and F are void of 1S, the immeasurable series limit or  $-E_1$ , B and F allow a simple conversion.

Precision at this level requires many significant digits. A fit of  $E_n$  [12] to 4<sup>th</sup> order in  $1/n$  through the origin, tested with terms in Table 1, gives slope  $1-1,79201817 \cdot 10^{-8}$  and intercept  $26940,95752/29979245,8=0,00008965361 \text{ cm}^{-1}$ . This results in the terms in Table 2. The conversion corresponds with a change of Erickson's 1977 Rydberg  $R=109737,3177 \pm 0,00083 \text{ cm}^{-1}$  [12].

Table 1 reveals that A, B and C are exactly reproduced. The small discrepancies for D, E and F are much lower than experimental uncertainties, 10 kHz for D and 21 for E in [20-21]. With the small error of 1,74 kHz for F removed, the error reappears for D and E (1,71 kHz). The small difference of 1,26 kHz for all terms caused by this correction justifies their omission in Table 2.

Table 1 Observed [10] and intervals from this work in kHz (with errors  $\delta$ ). Prediction of H  $1S$ - $3S$

Intervals <sup>a,b</sup>	Observed	This work	$\delta$ (kHz)	Ref. <sup>c</sup>
A. $1S$ - $2S$	2466061413187,07	2466061413187,07	0,00	[17,18]
B. $2S$ - $8S$	770649350012,00	770649350012,00	0,00	[19]
C. [ $1S$ - $8S$ ]	3236710763199,07	3236710763199,07	0,00	
D. $2S$ - $4S$ - $1/4(1S$ - $2S)$	4797338	4797334,20	-3,80	[20]
E. $2S$ - $6S$ - $1/4(1S$ - $3S)$	4197604	4197601,94	-2,06	[21]
F. [ $6S$ - $2S$ + $1/4(3S$ - $2S)$ ]	599734	599732,26	-1,74	
G. <b><math>1S</math>-<math>3S</math></b> predicted <sup>d</sup>	to be measured	<b>2922743278654,37</b>		[11]

<sup>a</sup> only B and derived F do not depend on 1S

<sup>b</sup> derived values between square brackets result from  $C=A+B$  and  $F=D-E$

<sup>c</sup> the four intervals A,B,D,E are used for metrology in [10]

<sup>d</sup> by the same argument, all other intervals  $nS$  in Table 1 are predicted with the relative accuracy to reference term B [19]

Referring to [11], the predicted H  $1S$ - $3S$  interval (G in Table 1,  $n=3$  in Table 2) is correct within 1,74 kHz, i.e. the largest error in Table 2.

A 4<sup>th</sup> order fit is still sufficient to fit all data accurately, when 15 significant digits are used.

$N_n = E'_n / (1/2e^2/r_H)$  plotted versus Euclidean variable  $x_E$  (27b) gives  $N_n$ , equal to

$$-0,000028651871617x_E^4 + 0,000042968542402x_E^3 + 1,000344034289810x_E^2 - 0,000000000165642x_E \quad (29)$$

For 19 terms 2S to 20S in Table 2, average errors of 0,11 kHz give a precision of  $1,6 \cdot 10^{-12}$  %. Small deviations  $\epsilon_n$  nevertheless increase with increasing  $n$  (which we discuss elsewhere).

H terms in Table 2 allow a check of Euclidean variable  $X_E$  (28) for internal Euclidean  $\varphi$ -symmetry.

Table 2 H 1S-nS: original  $E_n$  [12] and converted  $E'_n$  in  $\text{cm}^{-1}$ , terms  $T_n$  in kHz and deviations  $\epsilon_n$  with fitting to 4<sup>th</sup> order (29)

n	$-E_n$ ( $\text{cm}^{-1}$ )	$-E'_n$ ( $\text{cm}^{-1}$ )	$T_n$ (kHz)	$\epsilon_n$ (kHz)
1	109678,773704000	109678,77174307900	0	
2	27419,817835200	27419,81734379700	2466061413187,07	1,706
3	12186,550237200	12186,55001899660	2922743278654,37	0,139
4	6854,918845390	6854,91872213227	3082581563818,04	-0,078
5	4387,140880900	4387,14080222353	3156563684658,80	-0,097
6	3046,621950400	3046,62189584705	3196751430452,60	-0,083
7	2238,332451300	2238,33241135261	3220983339585,82	-0,065
8	1713,722059150	1713,72202861737	3236710763199,07	-0,050
9	1354,051221430	1354,05119731790	3247493423457,69	-0,038
10	1096,780974420	1096,78095487230	3255206191292,99	-0,029
11	906,430202530	906,43018635921	3260912763770,46	-0,022
12	761,652903990	761,65289037408	3265253077913,06	-0,016
13	648,982171840	648,98216020327	3268630861427,32	-0,012
14	559,581428918	559,58141885409	3271311028226,93	-0,008
15	487,457495457	487,45748665884	3273473249318,27	-0,005
16	428,429358101	428,42935033704	3275242868326,18	-0,003
17	379,508294780	379,50828787203	3276709484882,61	-0,001
18	338,511977355	338,51197116509	3277938523538,06	0,000
19	303,816802757	303,81679717463	3278978658687,20	0,001
20	274,194630876	274,19462581233	3279866709043,60	0,002
				average 0,124

## V. Probing internal $\varphi$ -symmetry for fractal H

A 4<sup>th</sup> order fit of accurate  $E'_n$  data in Table 2 exposes the contribution of Bohr's  $1/n^2$  theory

$$-E'_n = -4,368336200714/n^4 + 5,555412530899/n^3 + 109677,583783388/n^2 - 0,000015348196/n \quad (30)$$

Subtracting term  $1/n^2$  discloses accurately symmetry differences beyond Bohr theory

$$\Delta E'_n = (4,368336200714/n^2 - 5,555412530899/n) / n^2 \text{ cm}^{-1} \quad (31)$$

if the small  $1/n$  term is disregarded. Using  $E_1$  in Table 2 gives  $\Delta E'_n$ , shifted by  $1,18.../n^2$  (see [22]

for the analysis based on  $E_n$ ). The hidden parabola in (31) is obtained by adding  $(1/2 \cdot 5,5554 / \sqrt{4,3683})^2$

$= 1,32901^2 = 1,766268$ . This leads to a harmonic Rydberg  $R_{\text{harm}}$ , larger than  $R_\infty$  and  $R_1$  and as revealed

by power fit (4) above, equal to [22]

$$R_{\text{harm}} = 109677,583783 + 1,766268 = 109679,350051 \text{ cm}^{-1} \quad (32)$$

H symmetry equation (31) with  $R_{\text{harm}}$  becomes a perfect Mexican hat curve, i.e. quartic [23]

$$\Delta_{\text{harm}} = (4,368336/n^2 - 5,555413/n + 1,766268)/n^2 \text{ cm}^{-1} = 1,766268(1 - 1,572642/n)^2/n^2 \quad (33)$$

critical at  $n = 2.1, 572642/n \approx \pi \approx 4\varphi^{1/2}$  [23].

Fig. 2 illustrates quartics for  $R_{\text{harm}}$ ,  $R_{\infty}$  and  $E_1$  versus  $4\varphi^{1/2}/n-1$ . The Hund-type Mexican hat curve with  $R_{\text{harm}}$  (33) is a signature for left-right asymmetry for composite atom H [23], most likely also the missing link to rationalize in- and external H symmetries, including  $\underline{H}$  [22,23]. Using  $R_{\infty}$  to disclose internal H symmetries as in QED creates larger energy differences (see Fig. 2). With (33) accurate to order kHz, five-fold H symmetry is obvious, since the theoretical Euclidean symmetry parabola (28) is reproduced exactly by the experimental H data in Table 2.

In fact, all numbers in (33) are sufficiently close to Euclidean variables (27)-(28), i.e.

$$9\varphi^{1/2}/4 = 1,768840600 \quad (34)$$

$$2\varphi^{1/2} = 1,572302756 \quad (35)$$

transforming (33) in  $(9\varphi^{1/2}/4)(1 - 2\varphi^{1/2}/n)^2/n^2$  and (31) in  $(9\varphi^{1/2}/4)[1 - (1 - 2\varphi^{1/2}/n)^2]/n^2$ . For internal H symmetry (35), the difference is only 0,000338763, just like 0,000344 in (24). This proves that both in- and external H symmetries stem from chaotic/fractal behavior [4-5], Euclid's golden number [2-3] or Penrose's 5-fold symmetry [6], the most important, almost divine symmetry in nature [2-3].

## VI. Discussion

(i) Spectral H data accurately follow a closed form quartic in  $1/n$ . Unless for Lamb shifts, odd  $1/n$  powers are absent in Bohr  $1/n^2$  and QED theories. If observed data [13] had 5 decimals, the use of [12] could have been avoided, since all main intervals in Table 1 are assessable with [13]. Only the smaller intervals remain with an error using [13] for conversion (for F in Table 1, this error of 100 kHz suggests Kelly data [13] have a wrong 4<sup>th</sup> decimal for 4S and/or 6S).

(ii) Euclidean H harmony rests on algebra, overlooked for H parts, e.g. recoil [16], see Section II.2. Like Cagnac et al. [14], we find that that using  $\mu$  as in relativistic theory (Section III) is questionable.

(iii) In the  $H_2$  spectrum, natural asymptote  $1/2e^2/r_H \approx 78844,9 \text{ cm}^{-1}$  shows as ionic energy  $D_{\text{ion}} = e^2/r_H$  [16]:  $r_H$  is close to observed separation  $0,74 \text{ \AA}$  in  $H_2$  [24] and gives fundamental  $H_2$  frequency of  $4410 \text{ cm}^{-1}$  [24]. With  $r_H$  and  $\varphi$ , molecular  $H_2$  and atomic H spectra are intimately linked [16].

(iv) Incidentally, an angle of  $30^\circ$ , typical for Euclid's  $\varphi$ , also appears in the SM [25] as mixing angle for perpendicular interactions.

(v) Higher order terms in  $\xi = a/n$  or  $(1-\xi)$  brings H theory in line with Kratzer-type expansions like

$$E_n = a_0 \xi^2 (1 + a_1 \xi + a_2 \xi^2 + a_3 \xi^3 + \dots) \quad (36)$$

formally similar to but different than the more familiar Dunham expansion [26-30].

(vi) With the Sommerfeld-Dirac fine structure formula [31], the internal variable for H nP is  $1,5/n$ , rather than (35) for nS, which is responsible for the observed Lamb shifts [22, 31].

Euclidean H-symmetry, brought in by natural radius  $r_H$  is in line with the original Rydberg equation (1) and connects all H terms directly with its most important property, mass  $m_H$ . H is prototypical for atomic and molecular physics [16] as well as for fractal behavior, in line with Mandelbrot's views [4]. We do not expand on H structures, conforming to 5-fold symmetry [6], since Bohr's model is likely to be revised with classical physics, following the lines set out in Appendix A.

## VII. Conclusion

Although overlooked for a century, Euclidean H symmetry only shows when H mass is linked to its spectrum by its natural, classical radius  $r_H$ . A Hund-type Mexican hat curve for natural H proves that H is left-right asymmetric, which points to left- and right-handed states for composite hydrogen, say  $H$  and  $\underline{H}$  [22,23,29]. While this diverges from CPT-views on H [1], validating Euclidean  $\varphi$ -views on H rests, for a large part, on the value of H 1S-3S, to be measured in the near future [11].

## References

- [1] M. Amoretti et al., Nature 419, 456 (2002)
- [2] for references see [http://en.wikipedia.org/wiki/Golden\\_ratio](http://en.wikipedia.org/wiki/Golden_ratio) and <http://mathworld.wolfram.com>
- [3] M. Livio, *The Golden Ratio: The Story of Phi, the World's most Astonishing Number*, Broadway Books, New York, 2000; A. Stahkov, *The Mathematics of Harmony*, World Scientific Publishing, Singapore, 2008
- [4] B. Mandelbrot, *The Fractal Geometry of Nature*, Freeman New York, 1982
- [5] M.C. Gutzwiller, Phys. Rev. Lett. **45**, 150 (1980)
- [6] R. Penrose, *The Road to Reality*, Jonathan Cape, London, 2004
- [7] J.S. Rigden, *Hydrogen: The Essential Element*, Harvard University Press, Cambridge, 2002
- [8] M.I. Eides, H. Grotch and V.A. Shelyuto, Phys. Rept. **342**, 63 (2001)
- [9] J.R. Rydberg, Kungl. Svenska Vet. Handl. **11**, 23 (1889)
- [10] P.J. Mohr, B.B. Taylor and D.B. Newell, Rev. Mod. Phys. **80**, 633 (2008)
- [11] O. Arnoult et al., Can. J. Phys. **83**, 273 (2005)
- [12] G.W. Erickson, J. Phys. Chem. Ref. Data **6**, 831 (1977)
- [13] R.L. Kelly, *Atomic and ionic spectrum lines below 2000 Angstroms. Hydrogen to Krypton*. New York, American Institute of Physics (AIP), American Chemical society and the National Bureau of Standards, 1987
- [14] B. Cagnac et al., Rep. Prog. Phys. **57**, 853 (1994)
- [15] B. de Beauvoir, Eur. Phys. J. D **12**, 61 (2000)
- [16] G. Van Hooydonk, arxiv:0806.224
- [17] M. Fischer et al., Phys. Rev. Lett. **92**, 230802 (2004)
- [18] M. Fisher et al., Lect. Notes Phys., **648**, 209 (2004)
- [19] B. de Beauvoir et al., Phys. Rev. Lett. **78**, 440 (1997)
- [20] M. Weitz et al., Phys. Rev. A **52**, 2664 (1995)
- [21] S. Bourzeix et al., Phys. Rev. Lett. **76**, 384 (1996)
- [22] G. Van Hooydonk, Phys. Rev. A **66**, 044103 (2002)
- [23] G. Van Hooydonk, Acta Phys Hung NS **19**, 385 (2004)
- [24] K.P. Huber and G. Herzberg, *Molecular Spectra, Molecular Structure: Constants of Diatomic Molecules*, vol. IV, Van Nostrand-Reinhold, New York, 1979
- [25] P. Langacker, arxiv:0901.0241
- [26] G. Van Hooydonk, Z. Naturforsch. A **37**, 710 (1982)
- [27] G. Van Hooydonk, Spectrochim. Acta A **56**, 2273 (2000)
- [28] G. Van Hooydonk, Eur. J. Inorg. Chem., Oct., 1617 (1999)
- [29] G. Van Hooydonk, Eur. Phys. J. D **32**, 299 (2005)
- [30] G. Van Hooydonk, Phys. Rev. Lett. **100**, 159301 (2008)
- [31] G. Van Hooydonk, physics/0612141

Fig. 1  $nN_n$  versus  $1/n$  ( $\Delta$ ),  $1-1/n$  ( $\square$ ) (solid lines),  $1,5/n$  ( $+$ ) and  $1-1,5/n$  ( $\times$ ) (dashes).

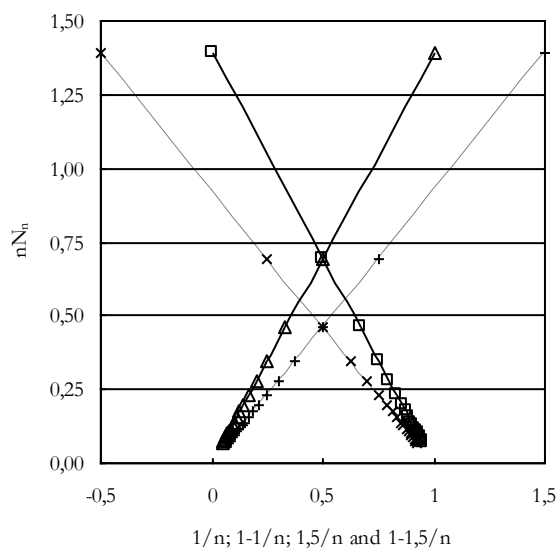
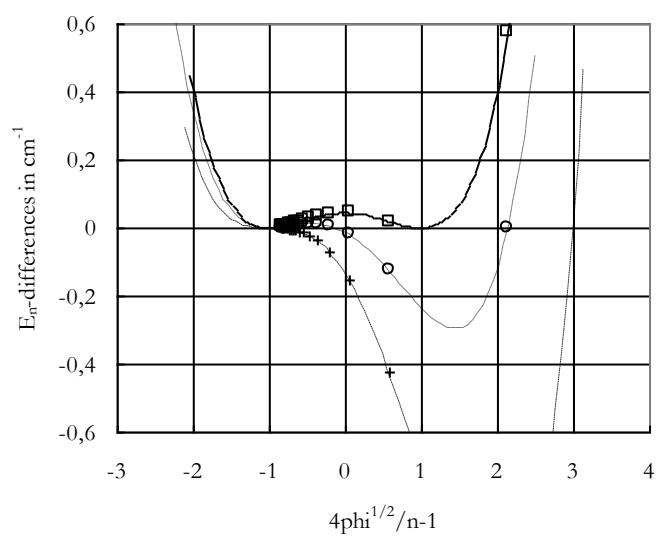


Fig. 2 Symmetry breaking curves in Euclidean H:  $E_n$ -differences (31)-(33) in  $\text{cm}^{-1}$  versus the appropriate Euclidean variable, see text): Mexican hat curve with  $R_{\text{harm}}$  (full-line  $\square$ ), with  $E_1$  (short dashes  $\circ$ ) and with NIST's  $R_\infty$  (broken dashes  $+$ )





## Appendix A Comparison of classical and Bohr H theories

This self-explanatory table contains all formulae for a stable charge-conjugated two particle Coulomb system, subject to periodic motion. Main results and differences are in bold.

Description	Classical H theory	Bohr H theory	#
Energy $E=T+V$	$E=1/2\mu v^2-e^2/r$	idem	A1
Hamiltonian	$E=1/2p^2/\mu-e^2/r$	idem	A2
Periodic motion	$E=1/2\mu\omega^2r^2-e^2/r$	idem	A3
Repulsive force d/dr	$\mu\omega^2r=\mu v^2/r=p^2/(\mu r)$	idem	A4
Attractive force d/dr	$e^2/r^2$	idem	A5
Equal forces (Newton)	$\mu v^2r=e^2$	idem	A6
Equal forces (Kepler, HO <sup>a</sup> )	$\mu v^2=e^2/r; \mu\omega^2=e^2/r^3; \omega^2=e^2/\mu r^3; \omega=\sqrt{k/\mu}$	vibrator or HO not considered	A7
Force constant $k_e$ at $r_e$	$k_e=e^2/r_e^3$	absent	A8
Constant periodicity $dE/d\omega$	$\mu\omega r^2=\mu v r=pr=C$	$\mu\omega r^2=\mu v r=pr=n\hbar$	A9
Moment	$p=C/r$	$p=n\hbar/r$	A10
Ratio A6/A9	$v=e^2/C$	$v=e^2/(n\hbar); v/c=e^2/(n\hbar c)=\alpha/n$	A11
H radius	$r=C/(\mu v)=C^2/(\mu e^2)$	$r=n\hbar/(\mu v)=n^2\hbar^2/(\mu e^2)=n^2r_B$	A12
Feedback of A10 in E (A1)	$1/2p^2/\mu-e^2/r=1/2\mu v^2-\mu v e^2/C=1/2C^2/(\mu r^2)-\mu e^4/C^2=1/2e^2C^2/(\mu e^2r^2)-e^2/r$	$1/2\mu v^2-e^2/r=1/2\mu e^4/(n^2\hbar^2)-\mu e^4/(n^2\hbar^2)=-1/2\mu e^4/(n^2\hbar^2)=-R_H/n^2$	A13
Feedback to $dE/dr=0$ at $r_0$	$-C^2/(\mu r^3)+e^2/r^2$ or $C^2/\mu=e^2r_0$	absent	A14
Feedback to E (A13)	$E=1/2e^2r_0/r^2-e^2/r=1/2(e^2/r_0)[(r_0/r)^2-2r_0/r]$	absent	A15
Feedback to $d^2E/dr^2=k$	$k=3C^2/(\mu r^4)-2e^2/r^3=3e^2r_0/r^4-2e^2/r^3=2(e^2/r_0^3)(r_0/r)^3[1,5(r_0/r)-1]$	absent	A16
Classical r definition using n	$r=nr_0$	absent, replaced by A12 or $r=n^2r_B$	A17
Plugging (A17) in k (A16)	$k_n=k_1(1/n^3)(1,5/n-1); k_1=e^2/r_0^3$	absent	A18
Plugging (A17) in E (A15)	$E=1/2(e^2/r_0)[1/n^2-2/n]$	absent	A19
Adding $E_0=1/2(e^2/r_0)$ to (A19)	$E'=E_0+1/2(e^2/r_0)[1/n^2-2/n]=E_0(1-1/n)^2$	absent	A20
Replacing $1/n$ by $(1-1/n)$	$E'=E_0[1-(1-1/n)]^2=E_0/n^2$	see result A13	A21
Energy difference, terms $T_n$	$T_n=E_0-E_0/n^2=E_0(1-1/n^2)$	$T_n=R_H-R_H/n^2=R_H(1-1/n^2)$	A22
Identical T formulae	n defined classically in (A17)	n in Bohr quantum hypothesis (A9)	A23

<sup>a</sup> HO is the classical Harmonic Oscillator

Force constant equations (A16)-(A18) for periodic motion and vibrations in HOs, are absent in Bohr theory. A switch to complementary variable (A21) is a switch from (i) energy  $V=-e^2/r$  in (A1) to energy difference  $\Delta V=-e^2/r+e^2/r_0$  and (ii) of moment  $p=C/r$  in (A10) to moment difference  $\Delta p=C(1/r-1/r_0)$ . Kinetic and potential energy differences give  $\Delta E=1/2(e^2/r_0)[1/2(1-1/n)^2-(1-1/n)]=1/2(e^2/r_0)/n^2$  (A21).

The usefulness of complementary variable  $1-1/n$  in (A21), usually not considered for H theory, is illustrated by respective 4<sup>th</sup> order fits (2 decimal version) of  $E'_n$  in Table 2

$$1/n: \quad E'_n = -4,37/n^4 + 5,55/n^3 + 109677,59/n^2 - 0,00/n + 0,00 \text{ cm}^{-1}$$

$$(1-1/n): \quad E'_n = -4,37(1-1/n)^4 + 11,91(1-1/n)^3 + 109668,05(1-1/n)^2 - 219354,37(1-1/n) + 109678,77 \text{ cm}^{-1}$$

Reducing H size classically in (A17) without a quantum theory gives the same results as Bohr's quantum hypothesis for angular momentum (A9).